COMPUTER DETERMINATION OF SEISMIC VELOCITIES — A REVIEW

By

J. F. MONTALBETTI*

ABSTRACT

During the past three years, the seismic exploration industry has given considerable attention to research and development of computer velocity analysis systems. Multifold ground coverage by seismic techniques such as the common depth point method provide a multiplicity of wave travel path information which allows direct determination of velocities associated with such paths. Appreciation of the difficulties encountered in determining appropriate dynamic corrections when well information is minimal or data quality too poor to allow a reliable T^2 - X^2 study of common depth point recordings so that primary energy will be stacked in phase, led to velocity determination using high speed digital computer facilities.

In this paper, the underlying principles of computerized velocity analysis will be reviewed. The velocities actually measured by such analyses and some of the commonly employed coherence measures such as crosscorrelation and semblance will be discussed to indicate their relationships to the input seismogram. A number of examples will be shown to demonstrate the performance of different techniques.

INTRODUCTION

During the past three years, the seismic exploration industry has given considerable attention to research and development of computer velocity analysis systems. Multifold ground coverage by seismic techniques such as the common depth point method provide a multiplicity of wave travel path information which allows direct determination of velocities associated with such paths. The effectiveness of the CDP method, among other factors, depends on applying the proper dynamic time corrections to the seismic data so that primary energy will be stacked in phase. Often in the past, these time corrections have been estimated from available well velocities in the vicinity of the prospect utilizing simple straight-ray or curved-ray methods, and of course have been applied with good success. The procedure however, becomes unsatisfactory when there is no well data available in the proximity of the prospect and because the velocity functions generated are for simple horizontally layered media, generally neglecting the effects of dipping horizons.

These problems can be remedied by subsequent application of residual normal moveout, or by a T^2, X^2 study of common reflection point traces. The method is however, somewhat limited by the seismic interpreter's ability to recognize and analyse visible strong reflectors and can become a particularly difficult task in poor record areas. Appreciation of these difficulties thus led to velocity determination using the digital computer.

*Research and Development Department,
Digital Technology (Calgary) Ltd., Calgary, Canada

In this paper, the underlying principles of computerized velocity analysis will be reviewed. The velocities actually measured by such analyses and some of the commonly used coherency measures such as cross correlation and semblance will be discussed to indicate their relationships to the input seismogram. A number of examples will be shown to demonstrate the performance of different techniques.

PRINCIPLE OF THE METHOD

Let us first consider a simple horizontally layered model as shown in figure 1. Common depth point traces gathered and displayed in order of their distance from the energy source will show a common reflection horizon as a hyperbola according to the familiar equation

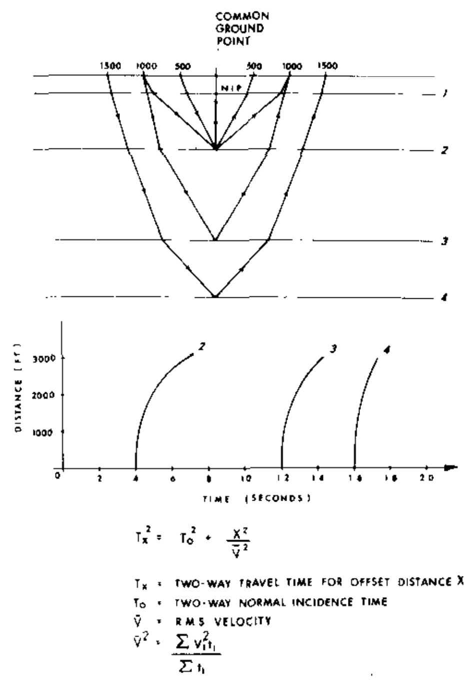

FIG. 1—Common depth point model for horizontal layering.

$$T_{x,n}^2 = T_{o,n}^2 + \frac{x^2}{\bar{V}_n^2} \tag{1}$$

where $T_{x,n}$ = two-way travel time for offset distance x and layer n,

$T_{o,n}$ = two-way normal incidence time for layer n,

$\bar{V}_n$ = RMS velocity,

These hyperbolic paths are shown in figure 1.

The RMS velocity is the same as that given by Dix (1955) and defined by

$$\bar{V}_n^{\,2} = \frac{\sum_{i=1}^{n} v_i^{\,2} t_i}{\sum_{i=1}^{n} t_i}, \qquad (2)$$

where v_i = interval velocity of the ith layer,

t_i = two-way normal incidence travel time in the ith layer.

This definition represents the time-weighted, mean-square velocity and is contrasted to the simple average velocity

$$V_{a,n} = \frac{\sum_{i=1}^{n} v_i t_i}{\sum_{i=1}^{n} t_i}. \qquad (3)$$

Expression (1) represents the "straight ray" approximation to the travel-time distance relationship for horizontal layering. Derivations of this expression leading to the RMS rather than average velocity definition can be found in the literature (Schneider and Backus (1968), Taner and Koehler (1969)). Experimental studies using computerized ray tracing (Robinson, 1970) have shown that equation (1) yields good results for the time-distance relationship and that the average velocity definition should hardly ever be given serious consideration. In fact, this definition will invariably over correct a seismic record as the estimated average velocity will always be lower than that actually encountered.

The more complicated case of dipping beds is shown in figure (2). A simple calculation for a single layer with velocity V and dip angle θ gives for the time-distance relationship in the common depth point configuration

$$T_x^{\,2} = T_o^{\,2} + \frac{x^2\cos^2\theta}{V^2}, \qquad (4)$$

where T_o is the normal incidence time below the common ground point. This expression defines a hyperbola which becomes flatter as θ increases, with an apparent velocity.

$$\bar{V} = \frac{V}{\cos\theta}. \qquad (5)$$

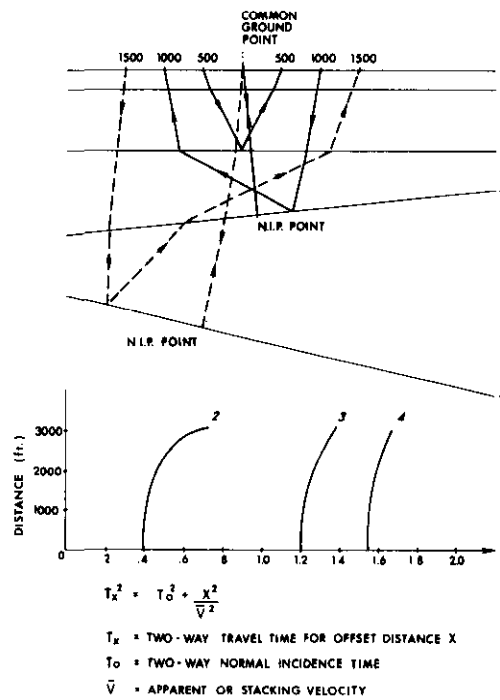

FIG. 2—Common depth point model for dipping layers.

Model experiments using different dips and interval velocities for multilayered media have indicated that arrival time-distance relations remain nearly hyperbolic so that we can define

$$T_{x,n}^{\;2} = T_{o,n}^{\;2} + \frac{X^2}{\overline{V}^2}, \tag{6}$$

where now, $\overline{V}$ represents the apparent RMS or stacking velocity. Appropriate choice of velocity $\overline{V}$ will thus define hyperbolic paths such as those shown in figure 2 so that proper corrections may be made when stacking the common depth point traces. In the most general form then, equation (6) expresses the time-distance relationship for the common depth point configuration with $\overline{V}$ representing the apparent RMS or stacking velocity.

Following these criteria, the principle of automatic velocity determination is shown in figure 3. At a particular normal incidence time T_0, a coherency measure is computed for various hyperbolic curves corresponding to a specified sweep of velocity $\overline{V}$ such that

$$V_1 \leq \overline{V} \leq V_2,$$

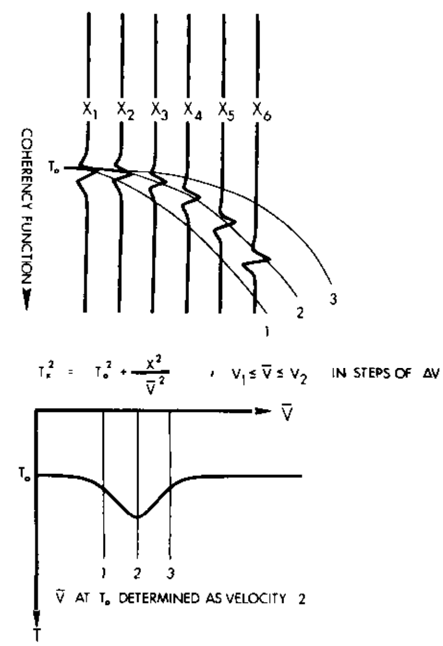

FIG. 3—Principle of computerized velocity analysis.

in constant velocity increments $\triangle\overline{V}$. This coherency is output for each velocity at that normal incidence time so that the maximum value of the coherency determines the apparent velocity of the particular event. By varying the T_o time an appropriate amount, a search such as this is carried out over the entire record length of interest so that a velocity function is determined.

COHERENCY MEASURES

In application of the principle of computerized velocity analysis, the coherency measure used can take many different forms. Since the main objective is to improve the stack of the common depth point traces, the actual composite can be used as a criterion for determining appropriate velocities. Define any digitized trace in a common depth point gather as $f_{i,t}$ where i refers to the channel index and t the time index. The trajectory across the gather corresponding to a particular velocity $\overline{V}$ will be given by t(i) so that the stacked amplitude for M input channels is given by

$$s_t = \sum_{i=1}^{M} f_{i,t(i)}. \tag{8}$$

This sum will exhibit a maximum when the trajectory t(i) corresponds to the correct apparent velocity $\overline{V}$, that is, when the events are properly aligned before addition. By successively correcting the seismic record with a sweep of known velocities and displaying the composite traces, an appropriate velocity function may be determined from the maxima of the stacked amplitudes.

A normalized version of the above expression can be written in terms of absolute amplitude variation as

$$\mathrm{COH} = \frac{\left|\sum_i f_{i,t(i)}\right|}{\sum_i \left|f_{i,t(i)}\right|} = \frac{\left|S_t\right|}{\sum_i \left|f_{i,t(i)}\right|} . \tag{9}$$

This expression will yield a value of unity if the traces have the same polarity or a value of zero if they are completely out of phase so that

$$0 \leq \mathrm{COH} \leq 1. \tag{10}$$

Many applications use cross correlation as a coherency measure. For each particular time T_0 and velocity $\overline{V}$, zero-lag cross correlation sums are computed over a window of some specified length T which is centered about T_0. The cross correlation sum is determined according to

$$\mathrm{T.CC} = \sum_t \sum_k \sum_i f_{i,t}\, f_{i+k,t(i+k)} , \tag{11}$$

where the summations over k and i refer to all possible channel combinations and the sum over t refers to the time window over which the cross correlation is computed. Equation (11) is an unnormalized cross correlation which can be written more simply as

$$\mathrm{CC} = \frac{1}{2} \sum_t \left[\left[\sum_i f_{i,t(i)} \right]^2 - \sum_i f_{i,t}^2 \right]$$

$$\mathrm{CC} = \frac{1}{2} \sum_t \left[S_t^2 - \sum_i f_{i,t}^2 \right] . \tag{12}$$

This expression shows the unnormalized cross correlation sum to be equal to ½ the energy difference between the "output" energy of the stack S_t and the gate input energy, where S_t is defined as in (8) along the trajectory of interest. Thus, if t(i) defines the trajectory of a coherent event across the input channels, the first term of equation (12) will be large with respect to the second and CC will exhibit maximum.

At this point, it is appropriate to consider normalization of equations (11) and (12). *The usual normalization of (11) can be determined* from a statistical approach so that the normalized cross correlation sum can be written

$$\mathrm{CC}^1 = \frac{2}{M\,(M-1)} \cdot \frac{1}{T} \sum_t \sum_k \sum_i \frac{f_{i,t}\, f_{i+k,t(i+k)}}{\sqrt{\sum_t f_{i,t}^2 \sum_t f_{i+k,t(i+k)}^2}} . \tag{13}$$

The constants introduced here ensure unit maximum amplitude so that the expression varies between $\pm$ 1 according to the likeness and phase of the signal across the channels. This expression is the most familiar normalized cross correlation measure, where the denominator can be considered to represent the geometric mean of the energy in the channels over the time gate chosen.

Neidell et al (1969) normalized expression (12) by the average trace energy rather than the geometric mean. If all the $f_{i,t}$ were equal then

$$CC = \frac{M\,(M-1)}{2} \sum_t f_{i,t}^2 \tag{14}$$

so that the energy normalized cross correlation sum is written

$$CC'' = \frac{\frac{1}{T} \cdot \frac{2}{M\,(M-1)} \cdot CC}{\frac{1}{T} \cdot \frac{1}{M} \sum_t \sum_i f_{i,t}^2} = \frac{1}{M-1} \; \frac{CC}{\sum_t \sum_i f_{i,t}^2}, \tag{15}$$

with

$$-\frac{1}{M-1} < CC'' \leq 1. \tag{16}$$

Computationally, expression (13) requires M/2 more multiplications than (15). Further, the statistically normalized cross correlation will give unit correlation if the phase and shapes of the signal are identical across the channels, even if the RMS signal amplitudes in each trace are different, while (15) will considerably penalize such variations. To understand this last observation more clearly, consider the cross correlation for two channels $f_{1,t}$ and $f_{2,t}$ which have identical shape but differ in amplitude by a scale factor $a < 1$ so that

$$f_{1,t} = f_t \qquad f_{2,t} = af_t \tag{17}$$

The statistically normalized cross correlation is given by

$$CC' = \frac{\sum_t f_t \cdot af_t}{\sqrt{\sum_t f_t^2 \cdot \sum_t a^2 f_t^2}} = \frac{a \cdot \sum_t f_t^2}{a \cdot \sum_t f_t^2} = 1, \tag{18}$$

while the energy normalized expression yields

$$CC'' = \frac{\sum_t f_t \cdot af_t}{\frac{1}{2}\left[\sum_t f_t^2 + \sum_t a^2 f^2{}_t\right]} = \frac{2a \sum_t f_t^2}{(1+a^2)\sum_t f_t^2} = \frac{2a}{1+a^2} \tag{19}$$

If, for example, $a = 0.5$

$$CC' = 1,$$
$$CC'' = 0.8, \tag{20}$$

so that the sensitivity to RMS amplitude difference is evident.

Another coherency measure often utilized in velocity analysis techniques considers the ratio of stacked trace energy to input energy. Using equation (8), this ratio is defined as

$$C = \frac{\sum_t \left[\sum_i f_{i,t(i)} \right]^2}{\sum_t \sum_i f^2_{i,t(i)}} = \frac{\sum_t s_t^2}{\sum_t \sum_i f^2_{i,t(i)}} . \tag{21}$$

If there are M identical data channels then

$$C = \frac{M^2 \sum_t f_t^2}{M \sum_t f_t^2} = M, \tag{22}$$

so that the normalized form of (21) becomes

$$C' = \frac{1}{M} \frac{\sum_t s_t^2}{\sum_t \sum_i f^2_{i,t(i)}} . \tag{23}$$

Physically then, (23) represents a normalized output/input energy ratio, with the output trace representing a simple composite of the input along the trajectory $t(i)$. It has values in the range

$$0 \leq C' \leq 1. \tag{24}$$

This coherency measure has been called the semblance coefficient (Neidell et al 1969) and is related to the energy normalized cross correlation function by

$$CC'' = \frac{1}{M-1} (M\, C' - 1). \tag{25}$$

Many other variations of these coherency measures are possible, each with its own advantages and limitations, but the above mentioned: variation is stacked amplitude, statistical and energy normalized cross correlation and semblance are those most often used in computerized velocity analysis techniques at this time.

APPLICATION OF THE METHODS

To illustrate use of the various coherency measures discussed, a 24-fold marine recording has been subjected to a number of different analyses. Figure 4 shows the results of a constant velocity analysis. In this process,

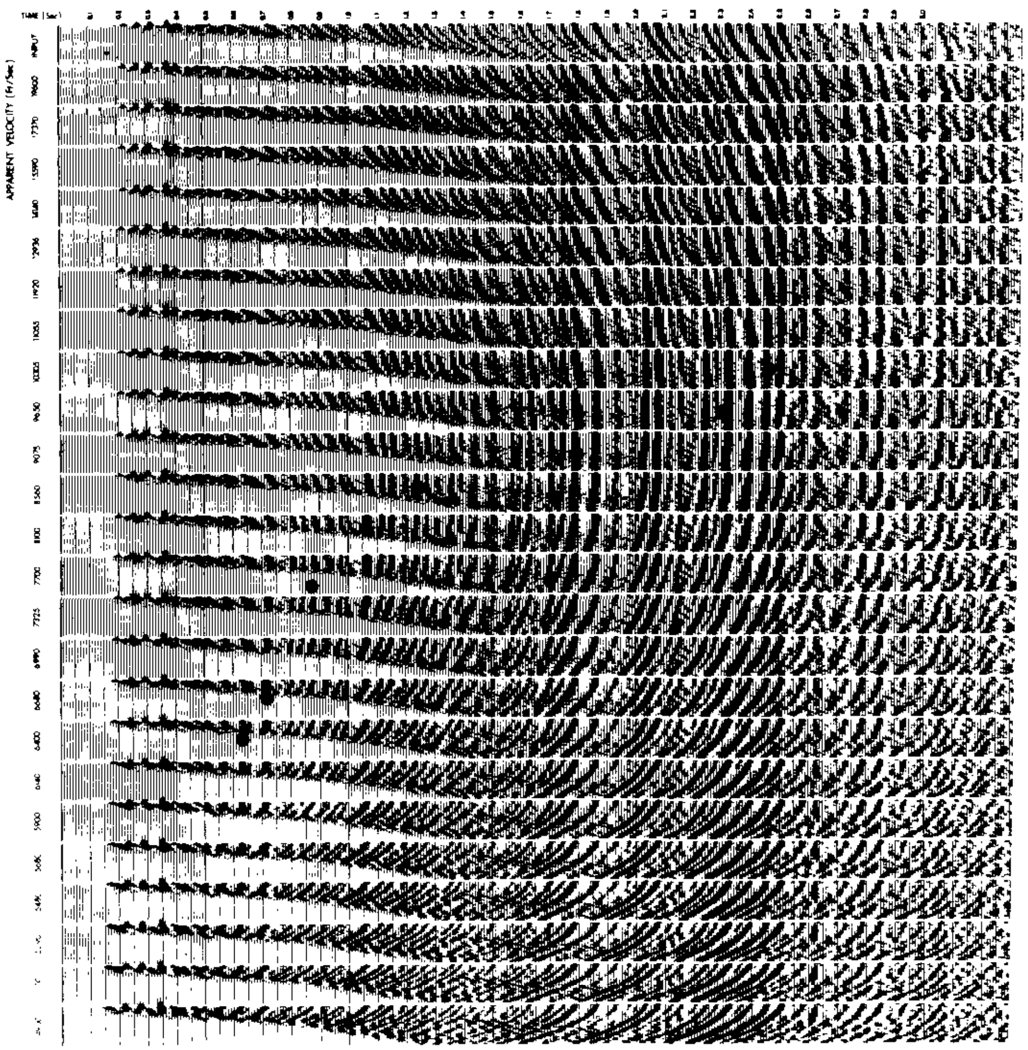

FIG. 4—Example of a constant velocity analysis applied to a 24-fold marine trace gather. The first record is the input seismogram followed by records corrected for a velocity scan from 19,000 ft/sec. to 4,900 ft/sec.

the record is corrected for a constant velocity and the result displayed for each velocity used. Alignment of an event at a particular record time indicates the proper correction velocity for that time. Picking alignments across the velocity scans thus allows determination of an appropriate function.

In the figure, the first record is the input seismogram followed by records corrected for a scan from 19,000 ft/sec. to 4,900 ft/sec. The output, similar in appearance to a harmonic analysis, can be used to pick a reasonable velocity function on good data as shown here, but the computer time involved and the fact that a complete record is output for each velocity are disadvantages. Since the velocity increments used are necessarily large, a rather coarse definition of stacking velocities is obtained. The process however, does give a good visual indication of the velocities encountered.

Figure 5 shows a constant velocity stack which is similar to the constant velocity analysis, except that after correction for a particular velocity, the traces are summed and the result displayed. This procedure illustrates use of the coherency measure given as equation (8) in the previous section. An interpretation has been made by picking the maximum amplitudes across the display and is shown by the solid curve. Picks from the previous constant velocity analysis are also indicated for comparison. The example clearly illustrates the fact that a fairly wide range of velocities will often provide adequate stacking amplitudes so that the interpretation should be made with considerable care if a more accurate velocity function is to be obtained. The technique demands considerably more computer time than the constant velocity analysis since a much finer velocity increment is used, but the visual compactness and this finer velocity scan are definite advantages.

Application of statistically normalized cross correlation as a coherence measure is shown in figure 6. In this process, computations were carried out over a 60 ms. time gate with increments of 20 ms. At each time, a sweep of velocities from 5,000 ft/sec. to 20,000 ft/sec. in 50 ft/sec. increments was performed and the correlation coefficients displayed. Use of the correlation technique as opposed to variation in stacked amplitude is clearly evident, as a velocity function is readily picked from this display. For comparision, picks from the constant velocity stack are also shown.

Figure 7 shows a comparison of four different coherence techniques: straight stack, absolute value sum, energy normalized cross correlation and semblance. In these processes, the coherency values were calculated for constant delta-T rather than constant velocity as in the previous example, and then output. A uniform delta-T increment was used along with a time-varying search range for computational efficiency. Each method shows to yield the same result in terms of the function defined, but generally sharper peaks are evident from the last two. The discriminating effect of energy normalized cross correlation with respect to RMS amplitude is clearly evident in the smear produced by the first break energy.

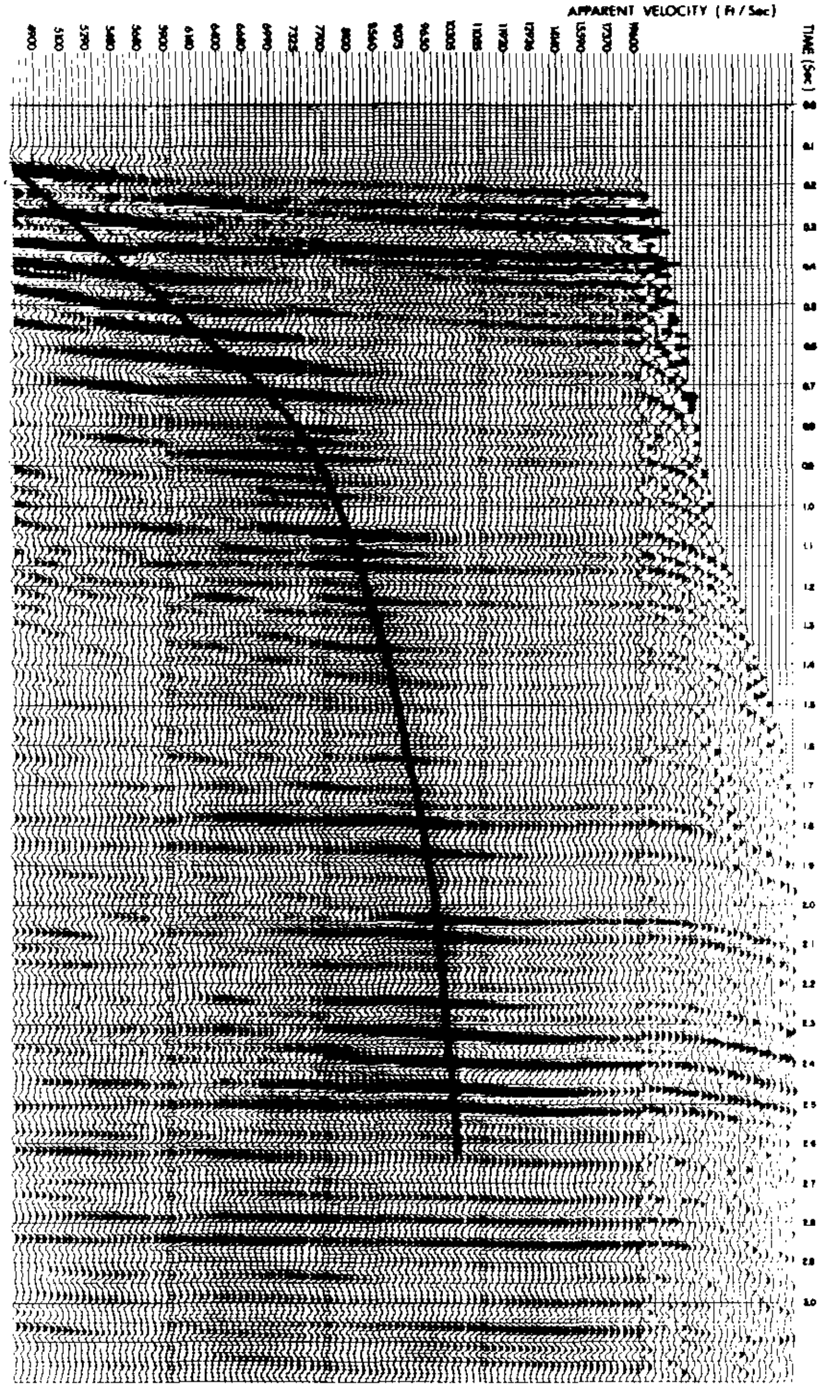

FIG. 5—Example of a constant velocity stack applied to the same record as in figure 4. The 24-fold input record is shown, followed by the stacked traces for each velocity used. This display demonstrates use of the coherency measure as given in equation (8).

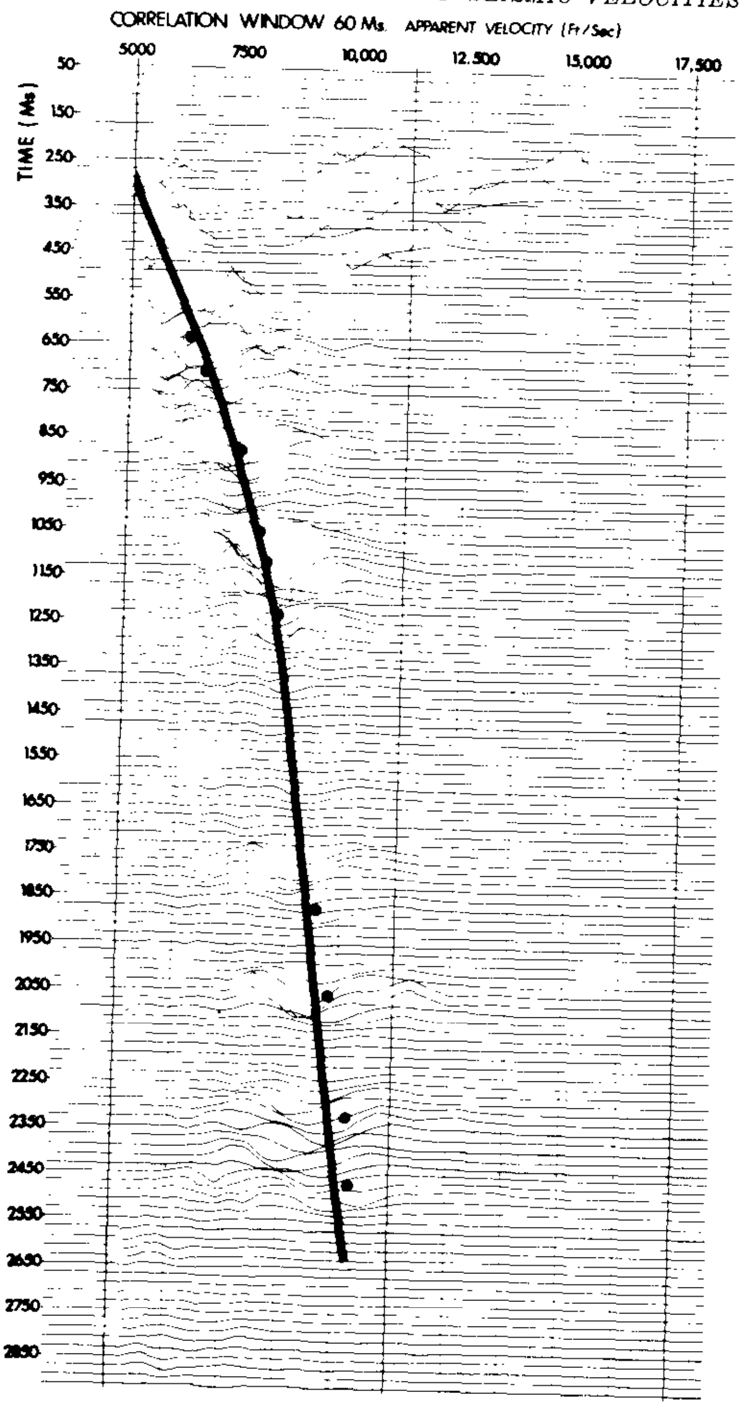

FIG. 6—Example of statistically normalized cross correlation as a coherence measure. A time gate of 60ms. with a 20ms. increment was used. At each time, a sweep of velocities from 5,000 ft/sec. to 20,000 ft/sec. in 50 ft/sec. increments was performed. The time-velocity axes are indicated. The input record was the same as in the previous examples.

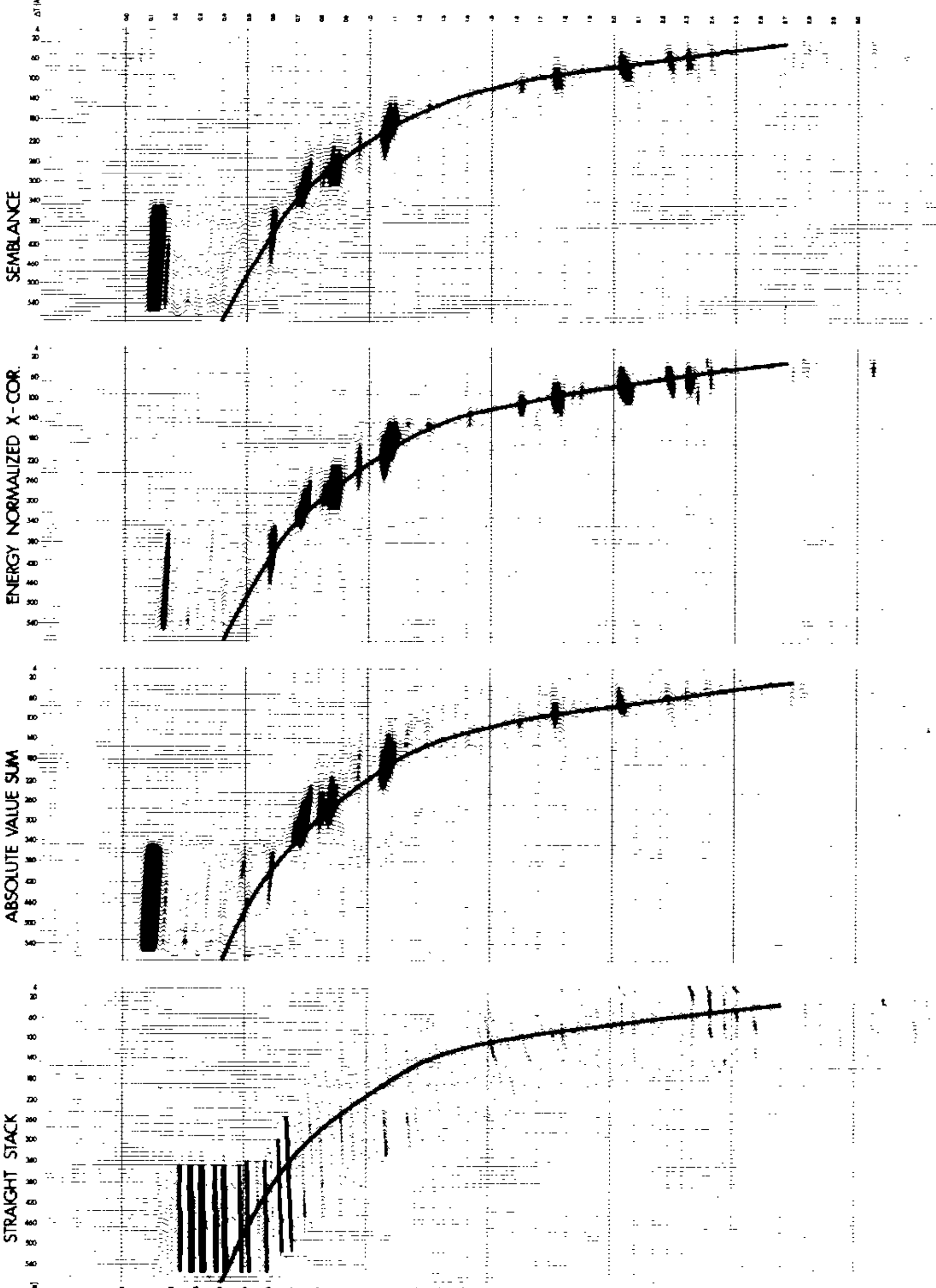

FIG. 7—A comparison of four different coherence techniques. In these examples, the coherency values were calculated at a constant delta-T search. Record time in seconds is indicated along the other axis. The input record was the same as in the previous examples.

CONCLUSION

The foregoing discussion has highlighted the principles of computerized velocity determination. Considerations have been given as to the meaning of the velocities measured by this process in terms of apparent RMS or stacking velocity. Following the definition of RMS velocity (equation 2), interval velocities may be obtained from an analysis using the well known relationship

$$v_n^2 = \frac{\bar{V}_n^2 T_{o,n} - \bar{V}_{n-1}^2 T_{o,n-1}}{T_{o,n} - T_{o,n-1}} \qquad (26)$$

where

v_n = interval velocity for the n^{th} layer

$\bar{V}_n$ = RMS velocity for the n^{th} layer

$T_{o,n}$ = two-way normal incidence time for the n^{th} layer

This calculation, although very simple to perform when time, velocity pairs are available, has often been exploited without proper attention given to dip, detector geometry and other factors which affect the apparent RMS velocity obtained from a computerized velocity analysis. Consideration of some of these problems has been discussed by Taner et al (1970).

A number of coherence measurements used in the application of velocity analysis techniques have been discussed and their performance on a 24-fold common depth point marine record shown by means of several examples. It is hoped that this review has clarified both the principles and application techniques of the computerized velocity analysis process.

ACKNOWLEDGEMENT

The author would like to thank Digital Technology (Calgary) Ltd. for permission to publish this work, and those staff who assisted in preparation of the examples shown.

REFERENCES

DIX, C. H., 1955, Seismic velocities from surface measurements: Geophysics, v. 20, p. 68 - 86.

NEIDELL, N. S., TANER, M. T. and KOEHLER, F., 1969, Semblance and other coherency measures for multichannel data: Presented 39th Annual International SEG Meeting, Calgary, Canada.

ROBINSON, J. C., 1970, An investigation of the relative accuracy of the most common normal - moveout expressions in velocity analyses: Geophys. Prosp., v. 18, p. 352 - 363.

SCHNEIDER, W. A. and BACKUS, M. M., 1968, Dynamic correlation analysis: Geophysics, v. 33, p. 105 - 126.

TANER, M. T., COOK, E. E. and NEIDELL, N. S., 1970, Limitations of the reflection seismic method; lessons from computer simulations: Geophysics, v. 35, p. 551 - 573.

TANER, M. T. and KOEHLER, F., 1969, Velocity spectra-digital computer derivation and applications of velocity functions: Geophysics, v. 34, p. 859 - 881.